Autonomous Optical Navigation for Landing on Target Point

Shunsuke Okada*,
Osamu Mori**, Jun'ichiro Kawaguchi**
Ken'ichi Shirakawa***, Takashi Kominato***

*The University of Tokyo
**Institute of Space and Science / Japan Aerospace Exploration Agency
***NEC Aerospace Systems, Ltd.

Abstract

This paper discussed the new optical navigation method for the landing mission of spacecraft. In November 2005, Hayabusa spacecraft touched down the asteroid 'Itokawa' twice. To navigate the spacecraft to the target point, new navigation software called 'GCP-NAV' was devised. GCP-NAV enabled high accurate position estimation of the spacecraft using the images which were taken at decent phase and geometrical model of Itokawa. In this method, operators at ground station estimated the position. Estimation by man enabled high accuracy and robustness. However there was problem of the delay caused by round trip time of radio wave between the earth and the asteroid, because the images for estimation need to be sent to the ground station. In this paper, we make the navigation process autonomously for real time control.

摘要

2005 年 11 月に探査機はやぶさは小惑星イトカワに 2 度のタッチダウンを行った．イトカワの表面は岩が多く，その着陸地点は非常に限定された．そのような極めて高精度な航法を実現するためにはやぶさの降下フェーズでは GCP-NAV と呼ばれる航法ツールが用いられた．GCP-NAV は事前観測によって得られたイトカワのモデルと降下時に撮像された画像上のイトカワとを比較し，探査機の位置を推定するものである．この GCP-NAV の特徴として画像とモデルとの比較を地上局のオペレータが行った点が挙げられる．イトカワの自転による太陽角が変化するような状況下においても人間は画像上から岩などの特徴点を抽出する能力が高いため，この手法は高精度かつロバスト性に優れていた．しかしながらこの手法では画像を一度地上局に送り，推定結果を探査機に送り返す必要があるため電波の往復時間による遅れが問題として挙げられていた．本研究ではこの遅れの問題を解決するために位置推定の作業を機上で行うことを目的として，自律的な推定手法を考案し，はやぶさ降下時に得られたデータを用いてシミュレーションを行いその有効性を検証した．

1. Introduction

In May 2003, Institute of Space and Science (ISAS) is launched asteroid explorer "Hayabusa". The main purpose of the mission is sample return from the asteroid "Itokawa". In November 2005 Hayabusa touched down the Itokawa twice. Its landing point was restricted by the safety of the spacecraft and the scientific requirement. Thus high accurate navigation and guidance were required. The decent phase was divided into two stages according to the altitude. When the altitude is less than 500m, called 'Final decent phase', the spacecraft descended toward the target marker which was dropped at rehearsal decent. On the other hand, when the altitude is 500~3000m, target range of this study, new developed navigation software 'GCP-NAV' was used [1]. GCP-NAV enabled high accurate position estimation of the spacecraft using the images which were taken at decent phase and geometrical model of Itokawa. The geometrical model was based on the observation at global mapping phase. The characteristic of GCP-NAV is that position estimation process is done by operators. Man can recognize landmarks on the image with robustness and accurately. For example, we can recognize the particular object even when light source is changed to some extent. GCP-NAV enabled high accurate navigation at decent phase. However there was problem of the delay caused by round trip time of radio wave between the earth and the asteroid, because the images for estimation need to be sent to the ground station. In the case of Hayabusa, the round trip time was approximately 30 minutes. Considering that decent speed of Hayabusa was 2~3m/s, in the worst case, it descended more than 100m during the round trip time. This delay problem becomes serious if the target celestial body is far from the Earth or the decent speed is fast.

The way to solve the delay problem is to make the

estimation process autonomously. In this paper, the outline of GCP-NAV is introduced in the section 2. The matching method is divided into two patterns according to the distance between the Hayabusa and the Itokawa. The autonomous algorithm for each pattern is proposed in the section 3 and 4. And in the section 5 the validity of the algorithm is tested by the computer simulation using actual data obtained at the decent phase.

2. GCP-NAV

2-1. Introduction of GCP-NAV

GCP-NAV is the navigation tool using at the decent phase. It determines the Hayabusa position using images taken by Optical Navigation Wide Camera (ONC-W), the attitude date of Hayabusa, and the GCPs position data. The GCPs position data were determined by observation at global mapping phase.

The matching method is divided into 2 patterns as follows:

1. Shape matching
2. Landmark matching

Method 1 and 2 are selected according to the distance between the spacecraft and the asteroid. Shape matching is used at far point, and Landmark matching is at near point.

2-2. Coordinate systems

The definitions of coordinates system are as follows,

- Inertia coordinate system: J2000. The origin is the Sun.
- HP coordinate system: $+z$ axis is toward the Earth, $+x$ axis is on the Itokawa-Earth-Sun plane and taken at the Sun side, and $+y$ axis is determined to complete right handed system. At the time of Hayabusa touchdowns, $+z$ is almost corresponded with altitude direction.
- ONC fixed coordinate system: ONC-W fixed coordinate. $+z$ axis points out of screen.
- HV coordinate system: 2 dimensional coordinate which shows the position on the image.

3. Shape matching

3-1. Outline

GCPs are located almost uniformly on the Itokawa's surface. When the asteroid size on the image is small i.e. the distance between spacecraft and asteroid is large, rough shape of the asteroid is recognized from the location of GCPs as shown in Fig. 1. The position vector from estimated spacecraft position to each GCP is calculated, and translated into HV coordinate. In the shape matching, the criterion is whether the size and the position of the asteroid on the image correspond with calculated GCPs' location at HV coordinate.

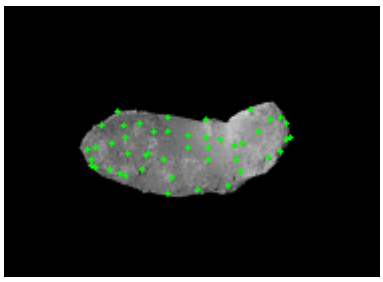

Fig.1 Shape matching

3-2. Selection of GCP

This subsection described about how to select GCPs which are used in the matching. The total number of GCP is 74. However some of them cannot be observed from spacecraft according to the relative position and attitude between the spacecraft and the asteroid. The observable conditions are that GCP is at spacecraft side and sunny side as Fig shows. Those conditions are shown in following equations.

$$\mathbf{v}_{ni} \bullet \mathbf{v}_{pi} > 0 \tag{1}$$

$$\mathbf{v}_{ni} \bullet \mathbf{v}_{SUN} > 0 \tag{2}$$

Where $\mathbf{v}_{ni}$ is a normal vector of i th GCP, $\mathbf{v}_{pi}$ is the vector form i th GCP to spacecraft, and $\mathbf{v}_{SUN}$ is the vector from the asteroid to the sun. If the shape of the target asteroid can be approximated the ellipsoidal body, the normal vector is calculated using position data as follows:

$$\mathbf{v}_n = \left[\frac{x_i}{a^2} \quad \frac{y_i}{b^2} \quad \frac{z_i}{c^2} \right]^T \tag{3}$$

Where a, b, c are the radii of target asteroid. This selection algorithm is also used in the landmark matching described in the next section.

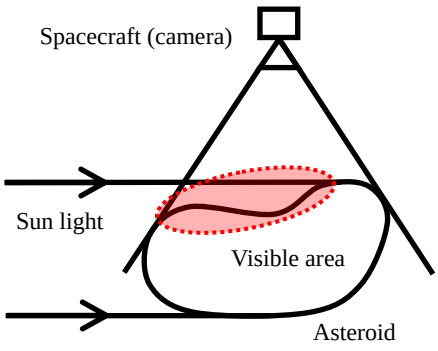

Fig.2 Selection of GCP

3-3. Algorithm

The procedure of the shape matching consists of

three steps.

① Binarize acquired image.

In this procedure the image is divided into two regions, asteroid region and the other (=space). The acquired image is binarized as follows:

$$H(i,j)=\begin{cases}0 & \text{On the asteroid}\\ 1 & \text{Out of asteroid}\end{cases} \tag{4}$$

Threshold gray level using at binarization is set as 20 (max gray level is 255).

② Calculate initial value for estimation.

Initial value $\mathbf{r}_{ek0}$ is calculated using the position of centroid of asteroid on the image (H_c, V_c), and estimated distance of previous step $\left\|\mathbf{r}_{e(k-1)}\right\|$.

$$\mathbf{r}_{ek0}=\left\|\mathbf{r}_{e(k-1)}\right\|\frac{\mathbf{r}_c}{\left\|\mathbf{r}_c\right\|} \tag{5}$$

$$\mathbf{r}_c=\begin{bmatrix} pH_c \\ pV_c \\ f \end{bmatrix} \tag{6}$$

where f is the focal length and p is the pixel pitch of ONC.

③ Estimate spacecraft position.

The criterion of estimation is smallness of the estimated distance $\left\|\mathbf{r}_{ek}\right\|$. When $\left\|\mathbf{r}_{ek}\right\|$ becomes minimum on the condition that all GCPs are on the asteroid on the image, the estimated position is regarded as the most probable position. The position of GCP at HV coordinate is calculated using information of the relative position and attitude between spacecraft and asteroid. Supposed that $\mathbf{r}_{HVi}$ shows the position of i th GCP on the image when the spacecraft is at the estimated position. N_{out}, the number of GCPs which are not on the asteroid in the image, is calculated as follows:

$$N_{out}=\sum_{i=1}^{N_{select}} H(\mathbf{r}_{HVi}(0),\mathbf{r}_{HVi}(1)) \tag{7}$$

Where N_{select} is number of GCPs selected in section 3-2.

4. Landmark matching

4-1 Outline

Shape matching is valid on condition that asteroid image size is smaller than whole image size. If a part of the asteroid runs out of the image area, the accuracy of the shape matching becomes worse. On the other hand, when the asteroid size on the image becomes large, landmarks on the asteroid surface become recognizable. Thus landmark matching is suitable at near point. In theory, minimum required number of GCP for the landmark matching is two. So the landmark matching is valid even when the asteroid runs out of image area. In the landmark matching, characteristic points are extracted from image, and compare with the GCPs position at HV coordinate. The criterion of this method is how many GCPs are at the extracted characteristic point.

4-2. Extraction method of landmark

In this subsection, how to extract landmark from acquired image is described. In GCP-NAV, rocks on the asteroid surface were set as landmarks. Man detects landmarks on the image using the information of change in a gray level. So to extract landmarks we should examine the change of gray level. In general, to examine the change of gray level, differentiation of image, for example gradient or Laplacian, is used [2]. Supposed that $f(i,j)$ shows the gray level at (i,j) element of the image. Horizontal gradient is shown as Eq. (8), and Laplacian is shown as Eq. (9).

$$D(i,j)=\frac{f(i,j+1)-f(i,j-1)}{2} \tag{8}$$

$$L(i,j)=f(i+1,j)+f(i-1,j)+f(i,j+1)+f(i,j-1)-4f(i,j) \tag{9}$$

Gradient and Laplacian have property similar to high pass filter. They are sensitive to change of value. As the spacecraft descend, details of the surface become observable. As a result, landmark candidates are increased, when differentiation of the image is examined. On the other hand, the landmark size of landmark varies according to the distance. So we need to pick up landmark with arbitrary size. In the other word, we hope to pick up the point with arbitrary special frequency.

Thus wavelet transform is adopted in this study. Wavelet transform is suitable to investigate frequency at arbitrary point in the signal along time or space [3]. The property and usage of the wavelet transform are described below.

At first, basis function (wavelet function) is shown as follows,

$$\psi_{a,b}(x)=\frac{1}{\sqrt{a}}\psi\left(\frac{x-b}{a}\right) \tag{10}$$

Where $\psi(x)$ is the function located near $x=0$, and whose mean is 0. a is parameter for dilation of $\psi(x)$, and b is that for shift. In the next step, to examine the frequency at arbitrary point of signal $f(x)$, correlation between $f(x)$ and $\psi_{a,b}(x)$ is

calculated with changing a and b. Eq. (11) shows wavelet transform of $f(x)$.

$$W(b,a)=\frac{1}{\sqrt{a}}\int_{\mathbf{R}} f(x)\overline{\psi\left(\frac{x-b}{a}\right)}dt \qquad (11)$$

Where $\overline{\psi(\bullet)}$ is complex conjugate of $\psi(\bullet)$. For the discrete signal, a and b change discretely. There are many types of wavelet function. In this study, we use Harr type wavelet (Eq. (12)) as a wavelet function.

$$\psi(x)=\begin{cases} 1 & (b\le x\le a+b) \\ -1 & (-a+b\le x<b) \end{cases} \qquad (12)$$

Fig. 3 shows the shape of the wavelet function.

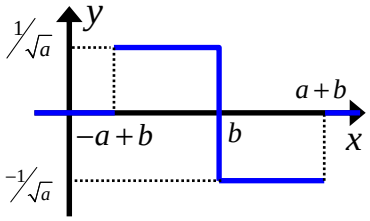

Fig. 3 Wavelet function (Harr)

Landmarks on the image correspond with the points where the correlation between image data and $\psi_{a,b}(x)$ is strong. Note that the image data has two dimensions. So in the 1 dimensional wavelet transform, examined direction (x direction of Fig. 3) can be set as arbitrary direction in the image. We examine the change of gray level to horizontal direction. The examined direction is related to the sun direction as explained below.

Fig. 4 shows simplified model of rock. Its shape is half sphere whose radius is 1. The sun direction is $-x$ and elevation angle is θ. Fig. 5 shows the normalized luminance value at the surface on this condition. The reflection is considered only diffuse reflection. The gray level of the image is proportional to luminance. Thus gray level changes from high to low along x axis of Fig. 4. And wavelet function changes from plus to minus as Eq. (12) shows. Thus if examined direction correspond with $+x$ direction of the Fig. 4, landmarks can be detected clearly. In the case of the decent phase of the Hayabusa, the sun direction is approximately negative horizontal direction at HV coordinate. So the examined direction is positive horizontal. If the sun direction is inverse, examined direction need to be inverse.

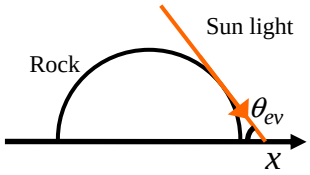

Fig. 4 Simplified model of landmark

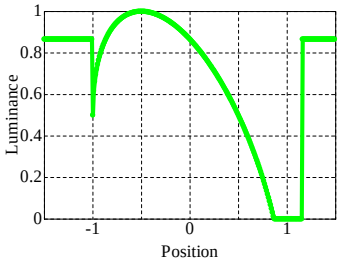

Fig.5 Luminance at the surface

In addition, strength of the correlation depends on a. As a becomes larger, the correlation with lower frequency becomes strong. The size of rock on the image relates to the frequency of image data. The special frequency near large rock tends to be low and near small rock tends to be high. Thus we consider that, landmarks with arbitrary size can be extracted as a is changed. To test this idea, we compute wavelet transform of Fig. 6, and extract top 15 large value areas (except for the rim of the asteroid) as Fig. 7 shows. In case (a), $a=1$ and in case (b), $a=4$. The areas enclosed by small square show the point whose value is large. Note that the small rocks pointed by arrow in case (a) are not extracted in case (b), and the large rocks pointed by arrow in case (b) are not extracted in case (b). Thus we can select the arbitrary size to some extent with coordinating the value of a. However the sizes of rocks on the image depend on not only real size but the distance from spacecraft. So a need to be changed according to the distance to extract a target landmark.

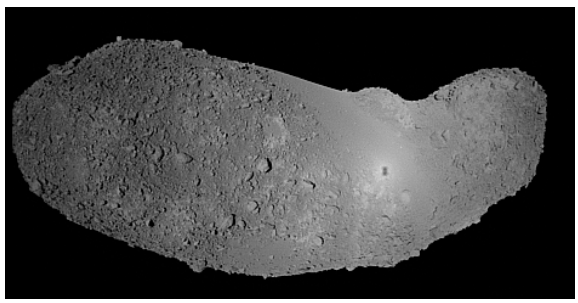

Fig. 6 Original image

(a) $a=1$

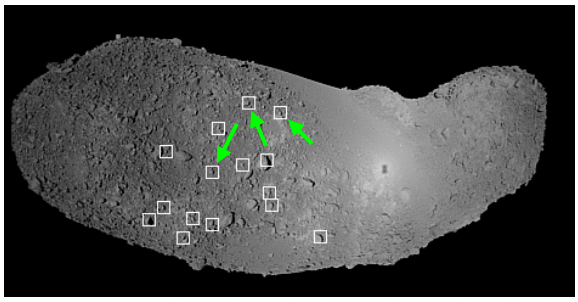

(b) $a=4$

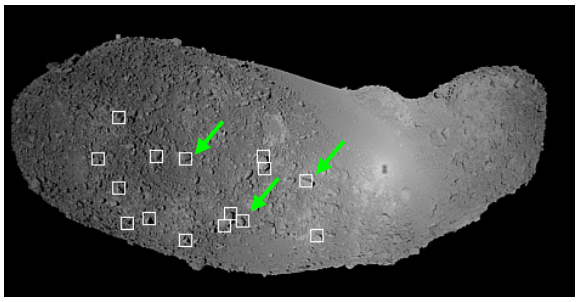

Fig. 7 Wavelet transform of Fig. 6

4-3. Evaluation function

In this subsection the estimation criterion is described. Supposed that $\mathbf{W}$ shows wavelet transformed data array of acquired image data. Evaluation function J_W is defined as follows:

$$J_W = \sum_{i=1}^{N_{select}} W(\mathbf{r}_{HVi}(0), \mathbf{r}_{HVi}(1)) \qquad (13)$$

Where N_{select} is number of GCP selected in section 3-2. J_W is calculated for estimated position in the search range. When J_W is minimum, the estimated position is regarded as the most probable position. The search range of x, y, z and search step depend on the interval of taking image, decent speed of spacecraft, computational capability, and required accuracy. Initial value of estimation at k th step $\mathbf{r}_{ek0}$ is calculated using estimated position and velocity at previous step as follows:

$$\mathbf{r}_{k0} = \mathbf{r}_{k-1} + \mathbf{v}_{k-1}(t_k - t_{k-1}) \qquad (14)$$

$$\mathbf{v}_{k-1} = (\mathbf{r}_{k-1} - \mathbf{r}_{k-2})/(t_{k-1} - t_{k-2}) \qquad (15)$$

Where t_k is the time when k th image is taken.

5. Simulation

In this section, the validity of the method described in section 3 and 4 is tested by computer simulation. In the simulation we use actual data, such as acquired image, attitude data of Itokawa and Hayabusa, and so on, obtained at decent phase in 19th and 25th November 2005. The estimation result is compared with the operation result of GCP-NAV. As mentioned above, the shape matching is valid at far point, and landmark matching is valid at near point. At first we use only shape matching. As a result the difference between the result of simulation and GCP-NAV expands when the altitude is less than 600m. And we can recognize landmarks on the asteroid from image when the altitude is less than about 1000m. Thus in the next step, matching method is switched from the shape matching to landmark matching when the altitude become less than 800m. The value of a is switched from 2 to 4 when the altitude is 600m.

Figs. 8 and 9 show the result of simulation and GCP-NAV. Fig. 8 shows the result of 11/19 and Fig. 9 shows that of 11/25 respectively. The difference between simulation and GCP-NAV is 50~100m for z, and about 10m for x, y at the shape matching altitude. And at the landmark matching altitude, the differences of three axes are all less than 20m.

In optical navigation, the accuracy of estimation for altitude direction is worse than that for in-plane position at far point. However for the landing mission, estimation of in-plane position is more important than that of altitude because the altitude is measured using LIDAR (Light Detection and Ranging). Thus the accuracy of the result is considered as acceptable level.

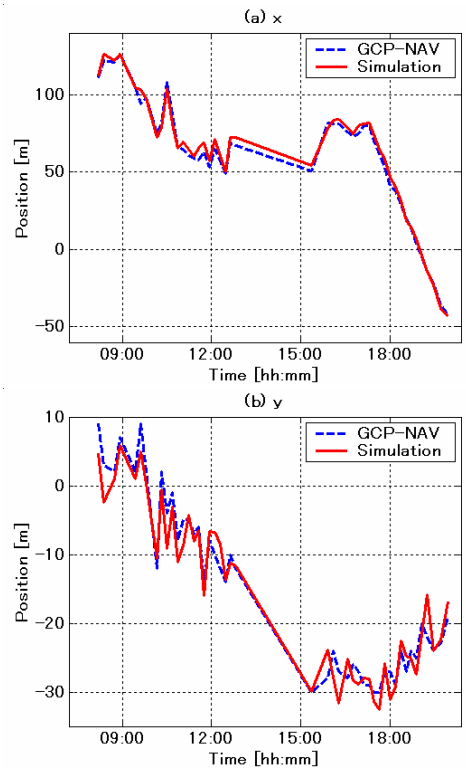

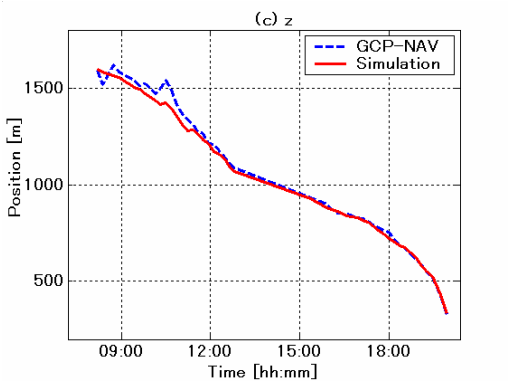

Fig.8 Simulation result (11/19)

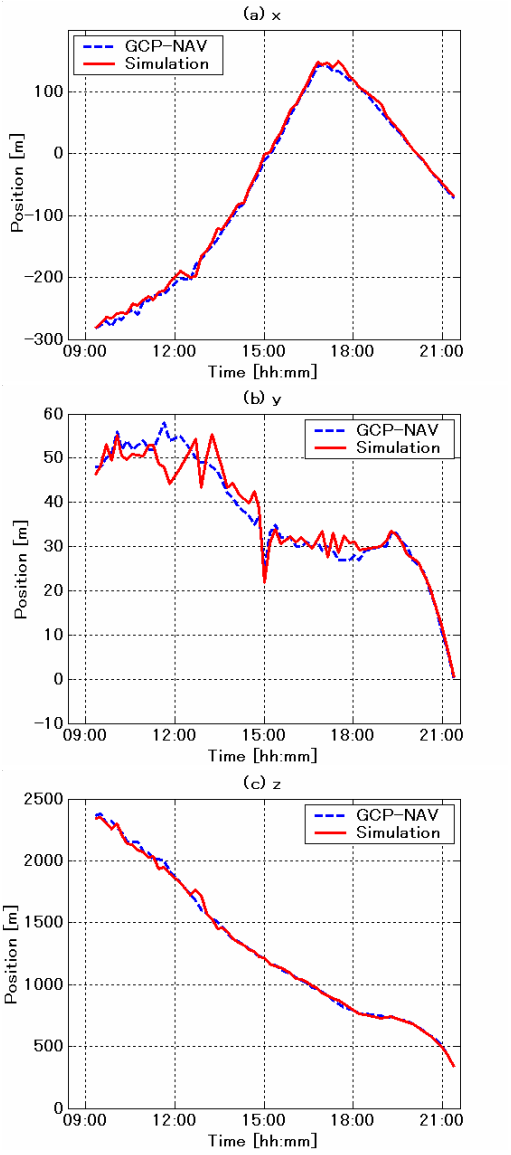

Fig.9 Simulation result (11/25)

6. Conclusion

The objective of this study is to make the navigation method using at decent phase of the spacecraft Hayabusa autonomously. The estimation method is divided into two patterns: the shape matching and landmark matching. Autonomous algorithms for two types are developed. In particularly, extraction process of landmark from the image is key point. In this paper wavelet transform is used to extract landmark. The proposed algorithm is tested by computer simulation using actual data obtained at the decent phase. The result of the simulation achieved acceptable accuracy for actual use in the mission.

Reference

[1]. Ken'ichi Shirakawa, Hideo Morita, Masashi Uo, Tatuaki Hashimoto, Takashi Kubota and Jun'ichiro Kawaguchi, "ACCURATE LANDMARK TRACKING FOR NAVIGATING HAYABUSA PRIOR TO FINAL DECENT", AAS-06-215, (2006)

[2]. Hideyuki Tamura, "Computer Image Processing", Ohmsha. Ltd, (2002)

[3]. Hiroki Nakano, Shizuo Yamamoto and Yasuo Yoshida, "Signal Processing and Image Processing using wavelet", Kyoritu Shuppan Co.Ltd, (1999)